Sensor validation of a Structural Health Monitoring Process for Aircraft Nacelle

Tristan Massot†, Mikhail Guskov†, Claude Fendzi†, Marc Rebillat†and Nazih Mechbal†

† PIMM Laboratory, UMR CNRS 8006 Arts et Métiers ParisTech,
151, Boulevard de l'Hôpital 75013, Paris, France

Abstract

This paper details the implementation process of an embedded structural health monitoring (SHM) system enabling condition-based maintenance of aircraft nacelles. One critical issue before being able to make use of such system is to ensure the effective bonding of the chosen actuators and sensors with their host structure, especially as the latter will be exposed to harsh environments and wide operational variability. In this work, we are concerned with the composite components of the nacelle and we use piezoelectric elements as both sensors and actuators. We propose an integrated approach that allows to validate a combination *"Substrate—Glue—Piezoelectric"* (SGP) and thus provides criteria to choose and size these assemblies. This validation scheme is based on the observation of the variations of the static capacity of the piezoelectric element after enduring various temperature and stress conditions when bonded to its host structure. Based on those SGP combinations, an active SHM strategy interrogating the structure by means of elastic wave propagation is currently being developed and preliminary results on samples representative of the nacelle are presented and discussed.

1. Introduction

Modern aircraft industry follows the general trend for optimizing structural performance especially in terms of strength to weight ratio. This implies, an increasing use of composite materials as well as the development of associated structural health monitoring (SHM) methods as these materials are more prone to damage than standard aeronautic materials [1, 2], . In that context, SHM systems are particularly important in order to ensure the required safety with the growing variability due to new materials and to compensate for the induced uncertainties that can generate penalizing costs due to planned maintenance [3]. As a component of an aircraft, the nacelles (that often include composite panels providing aerodynamic surfaces) hold a particular place. At the interface between the plane and the propulsion system, nacelles are exposed to both the outer and inner airflows as well as to the vibrations and high temperature flows due to the engine. In the same time, the presence of thrust reversers imposes high safety and reliability requirements on nacelles.

The development of SHM for aircraft composite structures is thus a necessary trend in the case of nacelles subject to strong environmental constraints. Several SHM methodologies have already been developed for this purpose and involve guided elastic waves in the analyzed structures [4], often making use of piezoelectric elements as sensors/actuators. But before being able to work with any of these SHM systems, the integration of the piezoelectric patches (and specifically their bonding) should be validated with respects to the host structures environmental conditions. To do so, electro-mechanical (EM) signature techniques have raised a real interest in the structural health monitoring community (see for example [1, 2, 3, 4, 5, 6]). The EM signature technique consists in measuring the EM signature of a piezoelectric element which is surface-mounted on a host structure in order to pinpoint incipient damages that may appear on the structure (damage detection) or to detect any damage on the sensor itself (sensor diagnostics). We are here particularly interested in detecting damage that can potentially occur on the sensor as a result of thermal or mechanical load.

The aim of the present work is thus to propose an approach validating a combination *"Substrate (host part material)—Glue—Piezoelectric element (sensor-actuator)"* (SGP) and to provide criteria that allows to choose and size these assemblies.

2. Host structures and thermal and mechanical environment

2.1. Tested specimens, piezo-electric elements, and glues

The specimens to be used in the present study are those representatives of the nacelle. Two components are of particular interest in the present work: the fan cowl outer panel made of monolithic carbon-fiber-reinforced polymer composites, and the inner fixed structure made of aluminum honeycomb core sandwich panels with carbon-fiber-reinforced polymer composites skins (see **Erreur ! Source du renvoi introuvable.**). Thus, two kinds of specimens with dimensions $400mm \times 300mm \times 31.4mm$ $(L \times l \times h)$ have been tested: sandwich specimens (see Figure *1*) and monolithic specimens (see Figure *2*).

Figure 1: Sandwich specimen

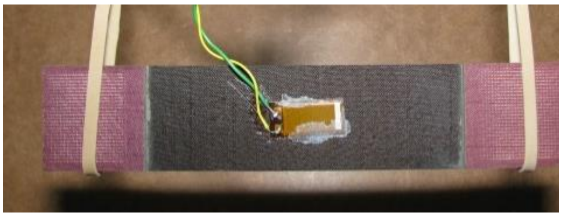

Figure 2: Monolithic specimen with a MFC

Furthermore, there exist two main technologies of piezo-electric elements that can be used for SHM purposes: rigid ones (PZT) and flexible ones (MFC). To validate the use of both types of elements, each specimen has been equipped with both. The PZTs (see Figure *3*) provided by Noliac are disc units while the MFCs (see Figure 4) provided by Smart Materials have a rectangular shape.

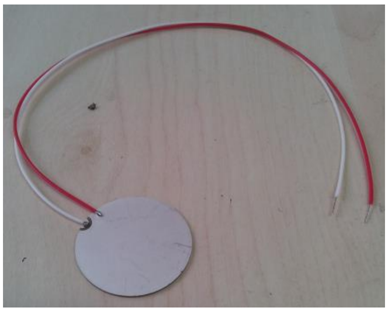

Figure 3: PZT disc from NOLIAC

Figure 4: MFC patch from SMART-MATERIALS

The glues that has been tested in this study and has been applied under pressure with use of vacuum bags is the Redux 322, a modified epoxy film adhesive able to operate from - 55 °C to 175 °C.

2.2. **Realistic nacelle thermal and mechanical environment**

The nacelle structure is subject to external solicitations including thermal and mechanical environmental flight conditions outside the aircraft and in the vicinity of the engine. Thermal load can be expressed in terms of temperature values ranging from $T_1 = -50°C$ to $T_2 = 100°C$.

Mechanical loads correspond to the sizing of the host parts and thus to the allowable of respective materials. In the context of bond assembly deformation compatibility, these conditions are to be expressed in terms of maximum strain magnitude ϵ, of order 10^{-3}. In order to validate a given SGP system, the observation of its response to these conditions is to be carried out in laboratory conditions.

2.3. Laboratory simulation of the thermal and mechanical environment

Mechanical loads are applied by conventional testing tensile/compressive machines: when the substrate strain is positive, the load is applied by means of a classical tensile test. For inducing negative strains, flexural tests are used. The size of the specimens is chosen at least double with respect to the specimens in order to avoid the influence of the samples boundary on the deformation of the assembly. Thermal loads are applied in a climatic chamber simultaneously with mechanical load when mounting configuration allows enough room for the chamber or separately when not possible. For monolithic specimens, tensile loads (Figure 5) are representative of the kind of mechanical load they are exposed to, and sandwich specimens undergo compressive loads (Figure 6) as they mainly endure this type of solicitation during flight.

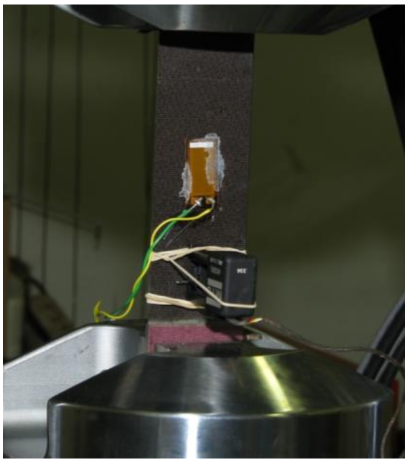

Figure 5: Tensile load of a monolithic specimen

Figure 6: Flexural load of a sandwich specimen at -60°C

3. Piezo-electric elements self-diagnostic

Sensor self-diagnostic procedures have been developed to be able to detect any damage occurring on the piezo-electric elements itself. Such procedures are based on the measurement of the electro-mechanical admittance of the piezo-electric element from which its static capacity is being extracted. This static capacity is afterward used as an indicator of debonding or failure of the piezo-electric element under study. This procedure has already been used to detect experimentally debonding and damages appearing on piezo-electric elements [1, 2, 3, 7, 8, 6]. This procedure has also already been used in aeronautical and spatial contexts [4, 5, 9] and is briefly recalled in what follows.

3.1. Admittance of a free piezo-electric element

The electric admittance $Y(\omega)$ of a piezo-electric element is defined as the ratio, in the frequency domain, of the current $I(\omega)$ over the tension $V(\omega)$ applied to that element. When the piezo-electric element is unbonded (and thus free to vibrate), its admittance $Y_l(\omega)$ is given as:

$$Y_l(\omega) = \frac{I(\omega)}{V(\omega)} = i\omega \times \frac{S}{t} \times \epsilon_{33} = i\omega C_l \qquad \text{Eq. (1)}$$

where S and t are the surface and the width of the considered element, and ϵ_{33} its dielectric permittivity. The static capacity of the free piezo-electric element is denoted C_l in what follows.

3.2. Admittance of a bonded piezo-electric element

If now we consider a piezo-electric element bonded to its host structure, its admittance $Y_c(\omega)$ can be approximated in the low frequency range by:

$$Y_c(\omega) = i\omega C_l[1-\kappa^2] = i\omega C_c \qquad \text{Eq. (2)}$$

Where κ^2 stands for the electromechanical coupling coefficient of the piezo-electric element and ranges between 0 and 1. C_c represents here the static capacity of the bonded piezo-electric element.

3.3. Sensor self-diagnostic procedure

The sensor self-diagnostic procedure proposed here is based on the analysis of the static capacities of a piezo-electric element given in Eq. (1) and Eq. (2). From these equations, it is straightforward to see that the electromechanical admittance of a piezo-electric element is a function of its geometrical parameters (S, t) and of its electromechanical coupling coefficient with the host structure κ^2. Thus, rewriting Eq. (2), a healthy piezo-electric element well bonded to its host structure will exhibit a static capacity given by:

$$C_c = \frac{S}{t} \times \epsilon_{33} \times [1-\kappa^2] \qquad \text{Eq. (3)}$$

Any damage on the piezo-electric element will manifest itself whether as a diminution of its usable surface S or of its dielectric coefficient ϵ_{33}. Thus, in case of damage the value of the product $S\epsilon_{33}$ will reduce to $\alpha S\epsilon_{33}$ with $0 < \alpha < 1$. A damaged piezo-electric element will thus have a static capacity given by:

$$C_c^E = \frac{\alpha S\epsilon_{33}}{t} \times [1-\kappa^2] = \alpha C_c < C_c \qquad \text{Eq. (4)}$$

It follows from Eq. (4) that any damage of the piezo-electric element can thus be detected as a lowering of its static capacity.

When debonding will occur on a piezo-electric element, its electromechanical coupling coefficient κ will be affected and will reduce to $\beta\kappa$ with $0 < \beta < 1$. The static capacity of a partially debonded piezo-electric element will thus be given as :

$$C_c^D = \frac{S}{t} \times \epsilon_{33} \times [1-(\beta\kappa)^2] > C_c \qquad \text{Eq. (5)}$$

From Eq. (5), the debonding of a piezo-electric element can thus be identified as an increase of its static capacity. And when the piezo-electric element will be totally debonded its static capacity will be equal to its static capacity when free, i.e. C_l, see Eq. (1).

It has thus been demonstrated that damage or debonding that can occur on a piezo-electric element manifest themselves as a decrease or an increase of its static capacity. A variation of the static capacity greater than a certain threshold will thus signify that a damage or a debonding has occurred after an environmental solicitation. However temperature variations can also be the source of static capacity variations. The threshold chosen to decide whether there is or not presence of damage or of debonding must thus integrate the eventual temperature variations encountered by the tested element in the laboratory between the different testing phases. Generally speaking, the daily range of temperature variations encountered in the laboratory are of the order of $10°C$ and the static capacity of piezo-electric element is expected to vary of 0.5 %/°C. A threshold of 5% has thus been chosen in what follows. Let C_c be the static capacity of a piezo-electric element after the first bonding and $\tilde{C}$ the static capacity of the same piezo-electric element after an environmental solicitation. We thus consider that there will be a significative event impacting the lifetime of the piezo-electric element (debonding or damage depending of the sign) if:

$$\frac{|\Delta C|}{C_c} = \frac{|\widetilde{C} - C_c|}{C_c} > 5\%$$ Eq. (6)

3.4. Electromechanical testing of the piezo-electric elements

The experimental setup used to realize the impedance measurements and to extract the static capacity according to Eq. (1) consists of a high speed data acquisition system, a waveform generator, a circuit able to measure both the voltage applied to the piezo-electric element and the resulting current, and a laptop. The whole experimental setup can be seen on Figure *7*. The voltage applied to the piezo-electric elements is a 250 ms long linear sine sweep having energy between 1 kHz and 400 kHz and the specimen rests with quasi free-free boundary conditions during the test.

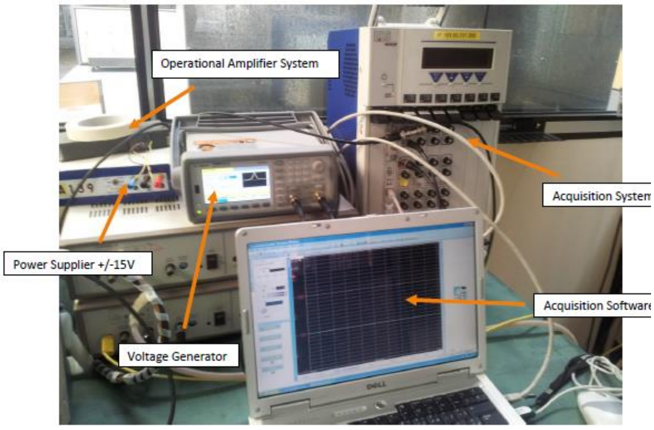

Figure 7: Impedance measurement setup

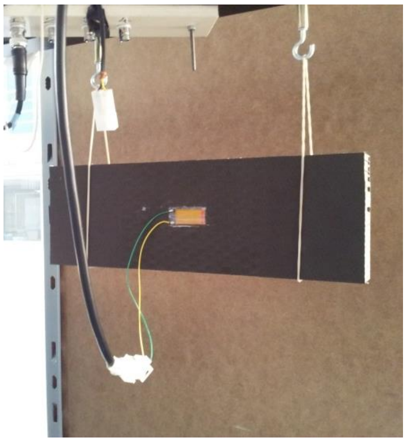

Figure 8: A sandwich specimen undergoing impedance measurement

4. Diagnostic and validation approach

4.1. Thermal and mechanical environmental loads

As stated previously, the operational objective is to ensure that the electromechanical signature of the assembled SGP features no variation above that due to the ambient temperature fluctuation. The above-mentioned aspects lead to a procedure for each specimen that can be summarized as in Figure *9*.

4.2. Typical results

The application of the above-described experimental plan yields to evolution of the electromechanical response of the system during the test. A typical example of such an evolution is given in Figure *8*. On this figure EM0 stands for the electromechanical test of the piezoelectric element alone and EM1 through EM6 for the tests during the loading stage of the assembled system. One can notice on the plot that the response in terms of admittance and capacity changes significantly at the moment when the assembly is bonded (between EM0 and EM1) as predicted by Eq. (1) and Eq. (2), but then the variation remains within 5% during the following thermal and mechanical load tests. This SGP configuration is thus validated here with respect to the chosen criteria.

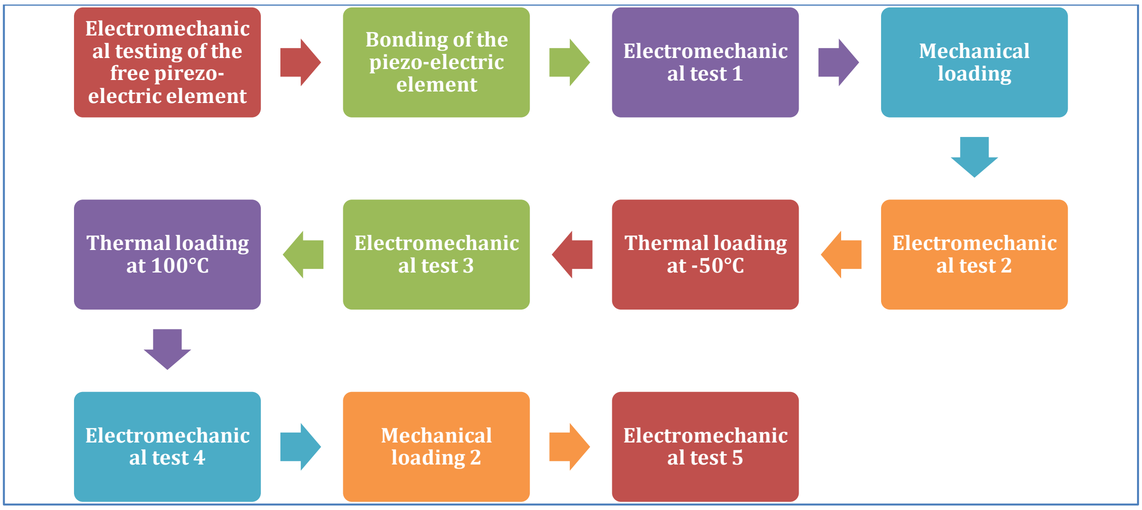

Figure 9: Experimental plan

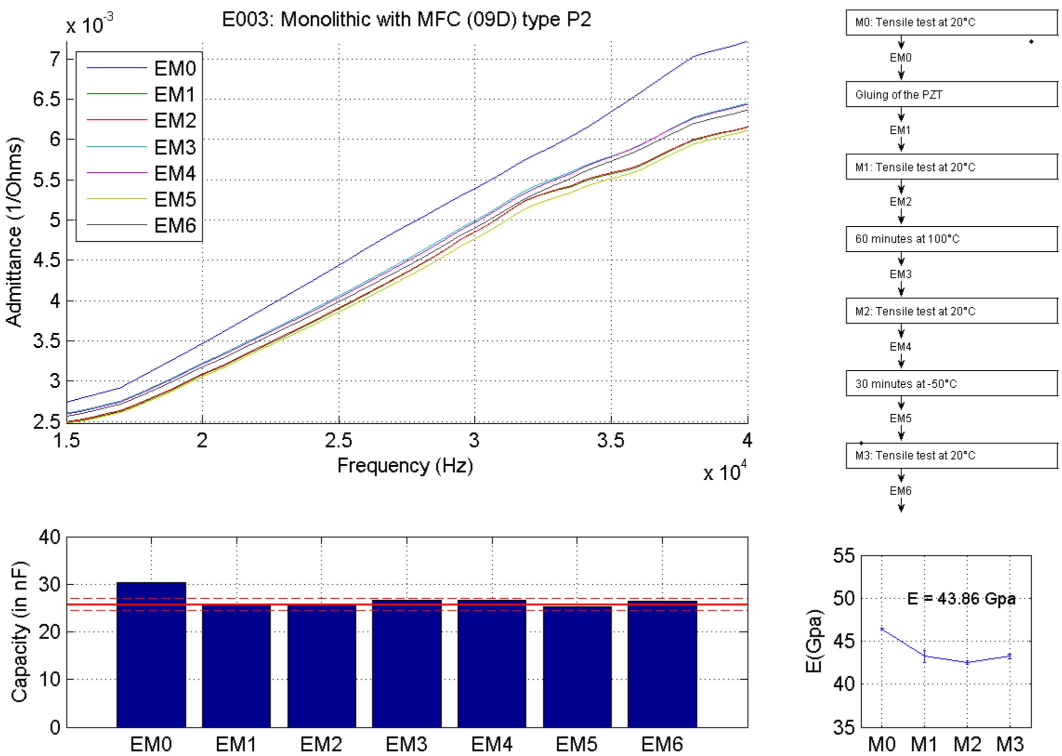

Figure 10: Evolution of electromechanical response of a monolithic specimen equipped with an MFC sensor/actuator

4.3. Overall results

In Figure 11, the results for two specimens for each considered case (monolithic and sandwich) are presented. In Figure 11, the results for two specimens for each considered case (monolithic and sandwich) are presented.

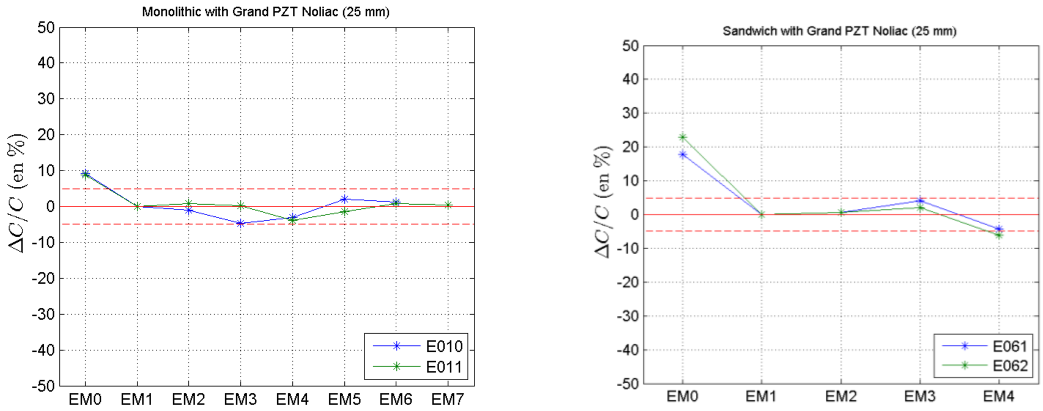

Figure 11: Results for PZT in case of monolithic and sandwich specimens

It can be seen that for all the possible SGP configurations, the static capacity variations stayed in the 5% safety range. We can thus conclude from those experiments that the different SGP that have been tested here satisfies the requirements of the present application.

5. Damage localization

SHM has been the topic of extensive research efforts over the last thirty years. This technology is now progressing toward operational service and several different techniques that depend on the structure's material, on the technology used for acting and sensing, on the position, size, and nature of damage may be employed. Among others, we can highlight vibration based approaches [14, 15] and more specifically the wave-based approaches that have the advantage to be sensitive to small flaws and offers the capability to monitor significant areas with few sensors [16]. We used in this work a probabilistic active SHM strategy based on the Time of flight of elastic wave propagation [4]. Time of flight is defined as the time lag between incident wave that the sensor first captures and the wave scattered by damage that the same sensor subsequently captures. The approach will be further outlined in a forthcoming publication. Here are some results for debonding and impacts damages localization.

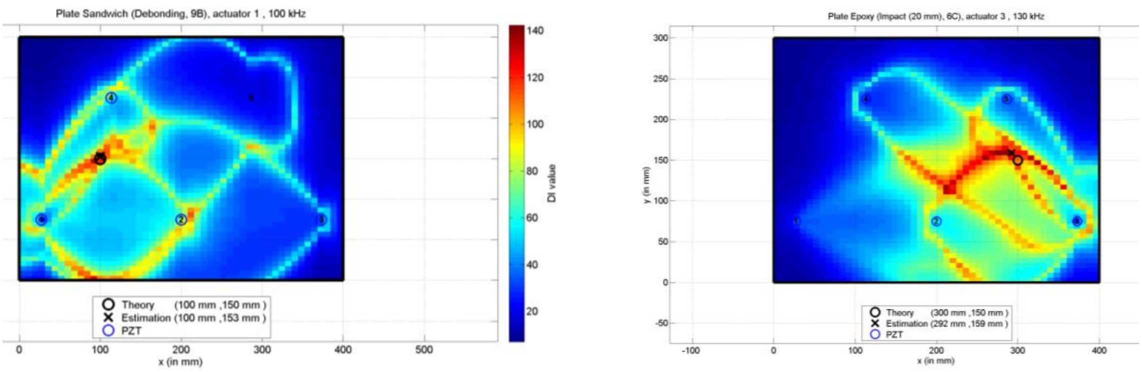

Figure 12: Damage imaging. The true damage position is market by a circle and the estimated by cross

6. Conclusion

In this work we have presented a procedure for the validation of piezoelectric element bonding on composite structures with respects to the host-structures operational environment. The application of this approach is presented on two different examples and it is shown how the chosen criteria can be used to discriminate unsuitable parameters combinations.

The solutions selected through this methodology offer the prospect of withstanding environmental conditions and allow for the SHM of aircraft nacelle structures, in particular by means of guided waves excited and measured by these piezoelectric components.

7. Bibliography

[1] F.-K. Chang, «Structural Health Monitoring: Condition-based Maintenance,» chez *8th International Workshop on Structural Health Monitoring (IWSHM)*, Stanford, 2011.

[2] W. J. Staszewski, C. Boller et G. R. Tomlinson, Health monitoring of aerospace structures: smart sensor technologies and signal processing, John Wiley and Sons, 2004.

[3] R. Hajrya et N. Mechbal, «Principal Component Analysis and Perturbation Theory Based Robust Damage Detection of Multifunctional Aircraft Structure,» *Structural Health Monitoring an International Journal*, 2013.

[4] S. Zhongqing, Y. Lin et L. Ye, «Guided Lamb waves for identification of damage in composite structures: A review,» *Journal of Sound and Vibration,* vol. 295, p. 753–780, 2006.

[5] G. Park, C. R. Farrar, A. C. Rutherford et A. N. Robertson, «Piezoelectric active sensor self-diagnostics using electrical admittance measurements,» *Journal of Vibration and Acoustics-transactions of the ASME*, vol. 128, pp. 469-476, 2006.

[6] G. Park, C. R. Farrar, F. L. di Scalea et S. Coccia, «Performance assessment and validation of piezoelectric active-sensors in structural health monitoring,» *Smart Materials & Structures*, vol. 15, pp. 1673-1683, 2006.

[7] S. Park, G. Park, C. B. Yun et C. R. Farrar, «Sensor Self-diagnosis Using a Modified Impedance Model for Active Sensing-based Structural Health Monitoring,» *Structural Health Monitoring-an International Journal,* vol. 8, pp. 71-82, 2009.

[8] S. G. Taylor, G. Park, K. M. Farinholt et M. D. Todd, «Diagnostics for piezoelectric transducers under cyclic loads deployed for structural health monitoring applications,» *Smart Materials and Structures,* vol. 22, 2013.

[9] Y. Zheng, C. Martinez, D. Easton, G. Park et K. Farinholt, «Sensor Self-Diagnostics for Piezoelectric Transducers Operating in Harsh Temperature Environments,» chez *Proceedings of SPIE Smart Structures and Materials & Nondestructive Evaluation and Health Monitoring Conference*, San Diego CA, 2011.

[10] B. L. Grisso et D. J. Inman, «Temperature corrected sensor diagnostics for impedance-based SHM,» *Journal of Sound and Vibration,* vol. 329, pp. 2323-2336, 2009.

[11] T. G. Overly, G. Park, K. M. Farinholt et C. R. Farrar, «Piezoelectric Active-Sensor Diagnostics and Validation Using Instantaneous Baseline Data,» *IEEE Sensors Journal,* vol. 9, pp. 1414-1421, 2009.

[12] V. Giurgiutiu et A. N. Zagrai, «Embedded self-sensing piezoelectric active sensors for on-line structural identification,» *Journal of Vibration and Acoustics-transactions of the ASME,* vol. 124, pp. 116-125, 2002.

[13] J. L. Blackshire et A. T. Cooney, «Characterization of bonded piezoelectric sensor performance and durability in simulated aircraft environments,» *Review of Progress in Quantitative Nondestructive Evaluation,* vol. 25, pp. 1694-1701, 2006.

[14] S. Chesné et A. Deraemaeker, «Damage localization using transmissibility functions: A critical review,» *Mechanical Systems and Signal Processing,* vol. 38, p. 569–584, 2013.

[15] K. Saeed, N. Mechbal, G. Coffignal et M. Vergé, «Artificial Neural Network Based Structural Damage Diagnosis Using Nonparametric Subspace Residual,» chez *7th International Workshop on Structural Health Monitoring, IWSHM*, Stanford (USA), 2009.

[16] Y. Liu, N. Mechbal and M. Vergé, "Damage monitoring based on wave illumination of structures," in *International Workshop on Structural Health Monitoring (IWSHM)*, Stanford, USA, 2011.